ELSEVIER

Chemical Geology 188 (2002) 23–32

CHEMICAL GEOLOGY
INCLUDING
ISOTOPE GEOSCIENCE

www.elsevier.com/locate/chemgeo

Estimation of surface precipitation constants for sorption of divalent metals onto hydrous ferric oxide and calcite

Chen Zhu *

Department of Geology and Planetary Science, University of Pittsburgh, Pittsburgh, PA 15260, USA

Received 29 June 2001; accepted 20 March 2002

Abstract

Equilibrium constants for modeling surface precipitation of divalent metals, M^{2+}, onto hydrous ferric oxide and calcite were estimated from linear correlations of standard state Gibbs free energy of formation, ΔG_f^o, of the surface precipitates. The experimental ΔG_f^o of the surface precipitates was derived from the surface precipitation model of Farley et al. [J. Colloid Interface Sci. 106 (1985) 226], which in turn was based on a surface complexation model coupled with solid solution representation for precipitation on the surface. The ΔG_f^o values are correlated through the relations

$$\Delta G^o_{f,\ M(OH)_2(s)} - 77.210\ r_{M^{2+}} = 1.03266\Delta G^o_{n,\ M^{2+}} - 305.368$$

and

$$\Delta G^o_{f,\ MCO_3(s)} - 83.991\ r_{M^{2+}} = 0.915\Delta G^o_{n,\ M^{2+}} - 343.331$$

where 's' stands for the end-member component of the solid solution, ΔG_f^o is in kcal/mol, r represents the Shannon–Prewitt radius of M^{2+} in a given coordination state (Å), and $\Delta G^o_{n,\ M^{2+}}$ denotes the non-solvation contribution to the Gibbs free energy of formation of the aqueous M^{2+} ion. The coefficients in the correlations were regressed from the aforementioned experimental ΔG_f^o. The statistically significant correlations (R^2=0.99) allow approximate estimation of free energies and, hence, equilibrium constants of the surface precipitation reactions for Be^{2+}, Mg^{2+}, Ca^{2+}, Mn^{2+}, Co^{2+}, Ni^{2+}, Sr^{2+}, Sn^{2+}, Ba^{2+}, Eu^{2+}, Ra^{2+}, Pb^{2+}, Hg^{2+}, Cu^{2+}, and UO_2^{2+}.

Keywords: Surface adsorption; Iron oxide; Calcite; Precipitation

1. Introduction

The surface precipitation model proposed by Farley et al. (1985) provides a thermodynamics construct for a continuum between surface complexation and bulk solid precipitation. The model predicts that, at low sorbate/sorbent ratios, surface complexation dominates. As the surface is loaded with sorbed ion, for example, divalent metal M^{2+} onto Hydrous Ferric Oxide surfaces (HFO, with a nominal formula of $Fe(OH)_3$; Dzombak and Morel, 1990), a surface precipitate is formed as a solid solution of $Fe(OH)_3$–$M(OH)_2$ (Fig. 1). With the increase of sorbate/sorbent ratios, both metal surface complexes and the mole

* Tel.: +1-412-624-8766; fax: +1-412-624-9662.
E-mail address: czhu@pitt.edu (C. Zhu).

0009-2541/02/$ - see front matter © 2002 Elsevier Science B.V. All rights reserved.
PII: S0009-2541(02)00060-8

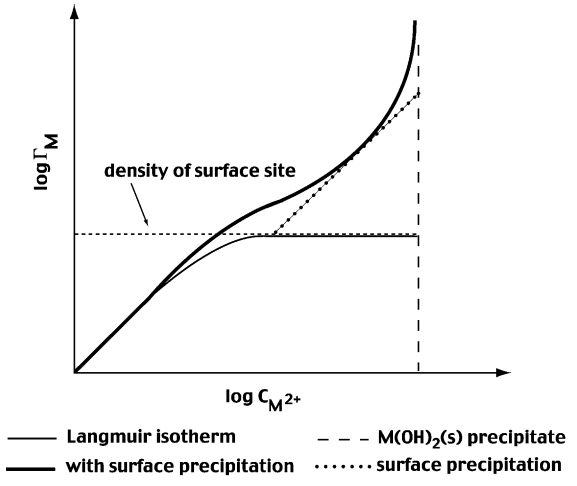

Fig. 1. Schematic representation of the idealized isotherms at constant pH. The total Fe concentration is fixed, as are the surface site concentrations in the system. The vertical axis indicates the surface concentration or sorption density (Stumm and Morgan, 1996), i.e., total metal sorbed on the surface per mol of HFO defined as,

$$\Gamma_M = \frac{[{=}MOH_2^+] + [M(OH)_2(s)]}{TOTFe}$$

As sorbate/sorbent ratios increase, surface sites are saturated with metal adsorbate and surface precipitate starts to form. Note that the vertical line labeled as "$M(OH)_2$(s) precipitate" should represent the solubility of the "hypothetical pure $M(OH)_2$ end member," not the "bulk solution precipitate" as indicated by Farley et al. (1985, Fig. 3). This is because the standard states for $M(OH)_2$(s) in the surface precipitation model are different from those for bulk precipitates; see text. A similar situation exists for surface precipitation onto calcite. The standard states for MCO_3 in the surface metals are (hypothetical) pure MCO_3 end-members with a calcite crystal structure, while the bulk precipitate may have an aragonite structure.

fractions of $M(OH)_2$ increase until all surface sites become saturated. At this point, surface precipitation becomes the dominant sorption mechanism. (The term "sorption" refers to all processes that transfer an ion from the aqueous to the solid phase. That includes surface adsorption or complexation, surface precipitation, bulk precipitation, and ion-exchange; Sposito, 1984). However, because the solubility of the solid solution component $M(OH)_2$(s) is far lower than the bulk $M(OH)_2$(s) at low mole fractions (see, e.g., Stumm and Morgan, 1981, 1996; Zhu et al., 1993, 1996), surface precipitation starts at an aqueous concentration of M^{2+} and a pH much lower than that for $M(OH)_2$(s). With increasing aqueous M^{2+} and pH, saturation with respect to bulk $M(OH)_2$(s) is approached.

The surface precipitation model has been used successfully to interpret experimental data at high sorbate/sorbent ratios for Zn^{2+}, Pb^{2+}, Cd^{2+}, Hg^{2+}, Cr^{3+}, and Cu^{2+} onto HFO (Farley et al., 1985; Dzombak and Morel, 1986, 1990; Charlet and Manceau, 1992; Karthikeyan and Elloitt, 1999), Cu^{2+} sorption onto hydrous aluminum oxide (Karthikeyan and Elloitt, 1999), Zn^{2+}, Mn^{2+}, Cd^{2+}, and Co^{2+} sorption onto calcite (Comans and Middelburg, 1987), and Co^{2+} sorption onto α-Al_2O_3 (Katz and Hayes, 1995). However, applications of the surface precipitation model are hampered by the lack of experimentally derived equilibrium constants.

On the other hand, tremendous progress has been made in developing empirical linear free energy correlations for crystalline solids (Sverjensky and Molling, 1992). Sverjensky and Molling (1992) proposed the following linear free energy relationship,

$$\Delta G^{o}_{f,\,MX} - \beta_{MX} r_{M^{2+}} = a_{MX} \Delta G^{o}_{n,\,M^{2+}} + b_{MX} \qquad (1)$$

where ΔG^{o}_{f} denotes the standard Gibbs free energy of formation for the solid MX, r represents the Shannon–Prewitt radius (Shannon, 1976) of M^{2+} in a given coordination state, and $\Delta G^{o}_{n,\,M^{2+}}$ denotes the non-solvation contribution to the Gibbs free energy of formation of the aqueous M^{2+} ion. The parameters a_{MX}, b_{MX}, and β_{MX} are regression parameters and are specific for each isostructural family of crystalline solids. This correlation formula is analogous to the well-known Hammett relationship for functional group substitution in organic compounds (Wells, 1968; Exner, 1988). The Sverjensky correlation has since been successfully applied to various crystalline structure families (Xu and Wang, 1999a,b,c; Xu et al., 1999; Wang and Xu, 2000). Recently, Wang and Xu (2001) applied this correlation formula to study the metal partitioning between carbonate minerals and aqueous solutions.

In this study, the Sverjensky linear free energy relationship was found to be applicable to experimentally derived standard state Gibbs free energy of formation, ΔG^{o}_{f}, of surface precipitates on HFO and calcite. The ΔG^{o}_{f} values were derived from equilibrium constants of surface precipitation reactions,

which are formulated based on the surface precipitation model that is linked to the surface complexation model (Farley et al., 1985; Dzombak and Morel, 1990). The empirical correlations developed in this study allow estimation of surface precipitation constants for Be^{2+}, Mg^{2+}, Ca^{2+}, Mn^{2+}, Co^{2+}, Ni^{2+}, Sr^{2+}, Sn^{2+}, Ba^{2+}, Eu^{2+}, Ra^{2+}, Pb^{2+}, Hg^{2+}, Cu^{2+}, and UO_2^{2+}, where experimental data are not available. Furthermore, the intrinsic equilibrium constants of surface complexation reactions involving surface precipitation are found to correlate linearly to the first hydrolysis constants of respective metals, similar to those found by Dzombak and Morel (1990) for surface adsorption only reactions.

Spectroscopic evidence for the formation of surface precipitates on HFO, as well as the precipitation mechanisms, was recently reviewed by Katz and Hayes (1995), Towle et al. (1997), and Ford et al. (1999). A variation to the Farley et al. (1985) thermodynamic model of surface precipitation was also proposed by Katz and Hayes (1995), which included intermediate multiple nuclear complexes and used the triple layer model of surface complexation. The subject of surface precipitation is an area of active research (see Katz and Hayes, 1995; Towle et al., 1997). Although more plausible spectroscopic evidence supports the formation of a MCO_3-calcite solid solution on calcite surfaces (see Sturchio et al., 1997 for review), metal sorption onto calcite surfaces appears to be complex at different conditions, and the calcite surface chemistry itself is a subject of active research (Stipp, 1999; Fenter et al., 2002). Thus, this communication evaluates the surface precipitation model as a theoretical construct. Whether the model is applicable to an individual metal, e.g., as a result of the ionic radius or ionic properties of the metal, thermodynamics cannot tell. Each case has to be evaluated individually and tested against bulk chemistry data on sorption as well as spectroscopic evidence.

2. Mathematical formulation and experimental data

2.1. Surface precipitation onto HFO

The presentation below of the surface precipitation model essentially follows Farley et al. (1985), Dzombak and Morel (1990), and Stumm (1992), but the model is described in a terminology and format more common in the geochemistry literature. The discussion focuses on calculating standard Gibbs free energy of formation for surface precipitates from the equilibrium constants of the surface precipitation reactions.

In the surface precipitation model of sorption of a divalent metal, M^{2+}, onto HFO, the surface adsorption reaction is rewritten as (Farley et al., 1985; Dzombak and Morel, 1990)

$$\equiv FeOH^{o} + M^{2+} + 2H_2O \rightleftarrows Fe(OH)_3(s) + {=}MOH_2^{+} + H^{+} \quad (2)$$

where the subscript 's' stands for a component of the solid solution $Fe(OH)_3$–$M(OH)_2$, symbols '≡' and '=' denote the bonds of metal atoms at the solid surface. $\equiv FeOH^{o}$ represents $[Fe(OH)_3]$ surface sites and $=MOH^{o}$ represents $[M(OH)_2]$ surface sites (Farley et al., 1985). At high surface coverage, the precipitation of M^{2+} and Fe^{3+} on the surface forms a solid solution of $Fe(OH)_3$–$M(OH)_2$ (Farley et al., 1985; Dzombak and Morel, 1990),

$${=}MOH_2^{+} + M^{2+} + 2H_2O \rightleftarrows M(OH)_2(s) + {=}MOH_2^{+} + 2H^{+} \quad (3)$$

$$\equiv FeOH^{o} + Fe^{3+} + 3H_2O \rightleftarrows Fe(OH)_3(s) + \equiv FeOH^{o} + 3H^{+} \quad (4)$$

The components of the solid solution obey the mass balance constraint

$$X_{Fe(OH)_3(s)} + X_{M(OH)_2(s)} = 1 \quad (5)$$

where X stands for the mole fraction of a component in the solid solution and are calculated from the equations

$$X_{M(OH)_2(s)} = \frac{[M(OH)_2(s)]}{[M(OH)_2(s)] + [Fe(OH)_3(s)]} \quad (6)$$

$$X_{Fe(OH)_3(s)} = \frac{[Fe(OH)_3(s)]}{[M(OH)_2(s)] + [Fe(OH)_3(s)]} \quad (7)$$

where the brackets, [ ], stand for the mole concentrations of components per liter of aqueous solution.

For an ideal solid solution, we have $a_i = X_i$, where a_i is the activity of the component i in the solid solution. Most bulk $M(OH)_2$ solids have a different structure from HFO. Additionally, the substitution is non-isovalent. The mixing in this type of solid solution is most likely nonideal (Towle et al., 1997). However, because $M(OH)_2(s)$ is in trace amounts for most applications, the assumption of an ideal solid solution is probably reasonable as long as a Henrian standard state for the trace end-member is defined. The Henrian standard state is defined as unit activity for hypothetical pure $M(OH)_2$ end-member of the solid solution with an HFO structure, extrapolated along the Henry's law slope from the infinitely dilute solution regions. A Raoultian standard state remains for the $Fe(OH)_3$ end-member, which is defined as unit activity for pure end-member component. As a result of such definitions, the activity coefficients for both $Fe(OH)_3$ and trace end-members are unity in the dilute solution regions where Henry's law is obeyed for the tracer (Ganguly and Saxena, 1987; Zhu and Sverjensky, 1992).

The mole balance equations for modeling surface adsorption now become (Farley et al., 1985; Dzombak and Morel, 1990):

$$\mathrm{TOTM} = \sum [\mathrm{M}^{2+}]_{\mathrm{aq}} + [{=}\mathrm{MOH}_2^+] + [\mathrm{M(OH)_2(s)}] \tag{8}$$

$$\mathrm{TOTFe} = \sum [\mathrm{Fe}^{3+}]_{\mathrm{aq}} + ([{\equiv}\mathrm{FeOH}^{\mathrm{o}}] - [{=}\mathrm{MOH}_2^+]) + [\mathrm{Fe(OH)_3(s)}] \tag{9}$$

$$\mathrm{TOT}({\equiv}\mathrm{FeOH}) = [{\equiv}\mathrm{FeOH}^{\mathrm{o}}] + [{\equiv}\mathrm{FeOH}_2^+] + [{\equiv}\mathrm{FeO}^-] + [{=}\mathrm{MOH}_2^+] \tag{10}$$

$$\mathrm{TOTH} = [\mathrm{H}^+] - [\mathrm{OH}^-] - [\mathrm{MOH}^+] - 2[\mathrm{M(OH)_2^o}] + [{\equiv}\mathrm{FeOH}_2^+] - [{\equiv}\mathrm{FeO}^-] + 2[{=}\mathrm{MOH}_2^+] - 2[\mathrm{M(OH)_2(s)}] - 3[\mathrm{Fe(OH)_3(s)}] \tag{11}$$

where the symbols TOTM, TOTFe, TOT(≡FeOH), and TOTH denote the total concentrations in a tableau representation of the system with M^{2+}, Fe^{3+}, ≡FeOH, and H^+ as components in the system. The summation sign stands for the sum of all aqueous species and complexes of M^{2+} or Fe^{3+}. ≡FeOH stands for surface site. Note, implied here is that all precipitated Fe is accounted for in the calculation of mole fractions in Eqs. (6) and (7), an assumption used by Farley et al. (1985) and Dzombak and Morel (1990) because of the open structure of Hydrous Ferric Oxides. A different formulation uses only the fraction of precipitated Al that forms the solid solution (Katz and Hayes, 1995).

Farley et al. (1985) used the above formulation to fit Cu^{2+}, Cd^{2+}, Pb^{2+}, and Zn^{2+} sorption experimental data of Benjamin (1978), based on the constant capacitance surface complexation model. They obtained a set of log K for reaction (3) (see Table 1). It is worth pointing out that these log K are different from those for the bulk $M(OH)_2$ solids not only in values, but also in concept. These are the solubilities of the end-member components of the solid solution. Pure or bulk divalent metal hydroxides, $M(OH)_2(s)$, can have different structures (Wells, 1984). A Henrian standard state for $M(OH)_2(s)$ means a hypothetical or "fictitious" pure $M(OH)_2$ end-member of the solid solution with an HFO structure.

From the log K of Farley et al. (1985) discussed above, we can calculate the standard state Gibbs free energy of formation for the end-members of the solid solution, $\Delta G^{\mathrm{o}}_{\mathrm{f,\ M(OH)_2(s)}}$. The standard state Gibbs free energy of reaction (3) can be calculated from

$$\Delta G^{\mathrm{o}}_{\mathrm{R}} = -2.303RT\log K \tag{12}$$

where K is the equilibrium constant for reaction (3), R is the gas constant, and T the temperature in Kelvin.

Table 1
Experimental and thermodynamic data for $M(OH)_2$–$Fe(OH)_3$ surface precipitates

M^{2+}	Log K	$\Delta G^{\mathrm{o}}_{\mathrm{R}}$	$\Delta G^{\mathrm{o}}_{\mathrm{f,\ M^{2+}}}$	$\Delta G^{\mathrm{o}}_{\mathrm{f,\ M(OH)_2(S)}}$	$\Delta G^{\mathrm{o}}_{\mathrm{n,\ M^{2+}}}$	$r_{\mathrm{M^{2+}}}$ (Å)
Zn^{2+}	−10.2	13,916	−35,170	−134,630	108,230	0.745
Cd^{2+}	−11.3	15,417	−18,570	−116,529	106,740	0.95
Hg^{2+}	−3.88	5,294	−71,372	−179,454	48,338	1.02
Cu^{2+}	−8.3	11,324	15,550,	−86,502	160,380	0.73
Pb^{2+}	−6.9	9,414	−5,710	−109,672	102,100	1.18

All free energy values are in cal/mol. Log K of reaction (3) from Farley et al. (1985) and Dzombak and Morel (1990); $\Delta G^{\mathrm{o}}_{\mathrm{f,\ M^{2+}}}$ and $\Delta G^{\mathrm{o}}_{\mathrm{n,\ M^{2+}}}$ Sverjensky and Molling (1992); and r^{2+}_{M} from Shannon (1976).

The standard Gibbs free energy of formation for the end-members is calculated from

$$\Delta G^{o}_{f,\ M(OH)_2(s)} = \Delta G^{o}_{R} + \Delta G^{o}_{f,\ M^{2+}} + 2\Delta G^{o}_{f,\ H_2O} - 2\Delta G^{o}_{f,\ H^{+}} \quad (13)$$

where $\Delta G^{o}_{f,\ M(OH)_2(s)}$ has a Henrian standard state as discussed above. The standard state for water is unit activity of pure water; for aqueous species other than H_2O, the standard state is unit activity of the species in a hypothetical 1 molal ideal solution referenced to infinite dilution at the temperature and pressure of interest. Table 1 lists the calculated Gibbs free energies.

2.2. Surface precipitation onto calcite

Comans and Middelburg (1987) applied the surface precipitation model of Farley et al. (1985) to sorption of divalent metals onto calcite. The reaction of M^{2+} adsorption onto calcite is written as

$$=CaCO^{o}_{3} + M^{2+} + HCO^{-}_{3} \rightleftarrows CaCO_3(s) + =MCO^{o}_{3} + H^{+} \quad (14)$$

and the precipitation of M^{2+} and Ca^{2+} on sorbent surface as

$$=MCO^{o}_{3} + M^{2+} + HCO^{-}_{3} \rightleftarrows MCO_3(s) + =MCO^{o}_{3} + H^{+} \quad (15)$$

$$=CaCO^{o}_{3} + Ca^{2+} + HCO^{-}_{3} \rightleftarrows CaCO_3(s) + =CaCO^{o}_{3} + H^{+} \quad (16)$$

The mass balance constraints require

$$TOTM = \sum [M^{2+}]_{(aq)} + [=MCO^{o}_{3}] + [MCO_3(s)] \quad (17)$$

$$TOTCa = \sum [Ca^{2+}]_{(aq)} + [=CaCO^{o}_{3}] + [CaCO_3(s)] \quad (18)$$

$$TOT(=CaCO_3) = [=CaCO^{o}_{3}] + [=MCO^{o}_{3}] \quad (19)$$

Based on the above formulation, Comans and Middelburg (1987) derived an isotherm equation for sorption onto calcite following Farley et al. (1985). From this isotherm equation, they retrieved log K of reaction (15) for Mn^{2+}, Cd^{2+}, Co^{2+}, and Zn^{2+}, using experimental data in the literature and based on the surface complexation model.

Through a similar exercise, elaborated on in the preceding section, the standard Gibbs free energies of formation for the MCO_3 components were derived (Table 2). A Henrian standard state is also adopted for MCO_3(s), as a hypothetical pure MCO_3 end-member with a calcite structure extrapolated from the dilute MCO_3 solid solution region. This is necessary because some divalent metal carbonates have the aragonite structure. Comans and Middelburg (1987) noted that their log K values are "apparent" solubility products because (1) the pH probably drifted in the experiments, compromising the use of the isotherm equation at fixed pH; and (2) an ideal solid solution for $(Ca, M^{2+})CO_3$ is assumed, which is not consistent with our knowledge of carbonate solid solutions (e.g., Lippmann, 1980).

3. Results and discussion

The ΔG^{o}_{f} values for the surface precipitates derived in the preceding section allow development of linear free energy correlations. A multiple linear regression analysis was performed based on Eq. (1) and using the parameters listed in Tables 1 (excluding Hg) and 2.

Table 2
Experimental and thermodynamic data for MCO_3–$CaCO_3$ surface precipitates

M^{2+}	Log K	ΔG^{o}_{R}	$\Delta G^{o}_{f,\ M^{2+}}$	$\Delta G^{o}_{f,\ MCO_3\ (S)}$	$\Delta G^{o}_{n,\ M^{2+}}$	$r_{M^{2+}}$ (Å)
Zn^{2+}	2.9	−3957	−35,170	−179,409	108,230	0.745
Cd^{2+}	4.9	−6617	−18,570	−165,469	106,740	0.95
Mn^{2+}	4.3	−5867	−55,200	−201,349	81,260	0.82
Co^{2+}	7.0	−9551	−13,000	−162,832	131,350	0.735

All free energy values are in cal/mol. Log K of reaction (15) from Comans and Middelburg (1987); $\Delta G^{o}_{f,\ M^{2+}}$ and $\Delta G^{o}_{n,\ M^{2+}}$ from Sverjensky and Molling (1992); and r^{2+}_{M} from Shannon (1976).

The following correlations are found for surface precipitates on HFO:

$$\Delta G^{o}_{f,\ M(OH)_2(s)} - 77.210\ r_{M^{2+}} = 1.03266\Delta G^{o}_{n,\ M^{2+}} - 305.368 \quad (20)$$

and on calcite:

$$\Delta G^{o}_{f,\ MCO_3(s)} - 83.991\ r_{M^{2+}} = 0.915\Delta G^{o}_{n,\ M^{2+}} - 343.331 \quad (21)$$

where ΔG^{o}_{f} is in kcal/mol, r represents the Shannon–Prewitt radius of M^{2+} in a given coordination state

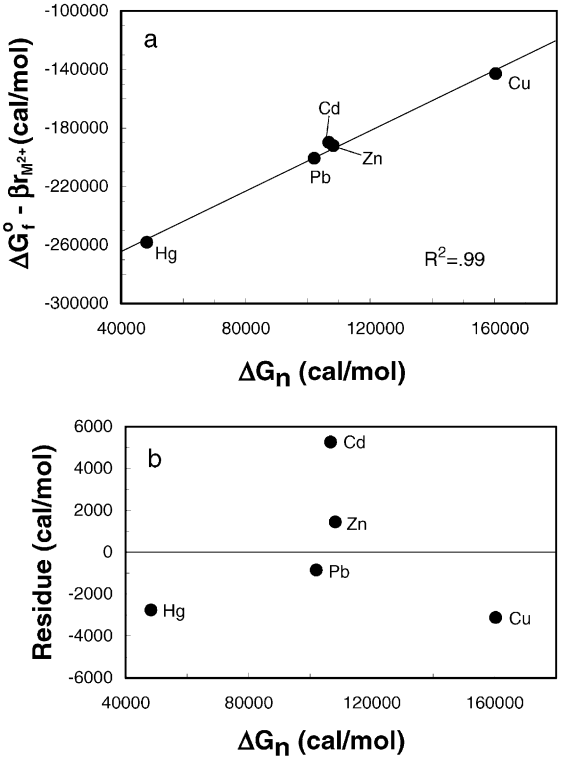

Fig. 2. (a) Multiple linear regression. The symbols represent experimentally derived values of the standard Gibbs free energies of formation for surface precipitates from Table 1. The vertical axis shows the left side of Eq. (1). (b) Residuals between experimentally derived G^{o}_{f} and values calculated from Eq. (20). The value for Hg is from Dzombak and Morel (1990), who used a diffuse double layer model and two types of surface sites to deduce the experimental data. This value was not used in regression, but it is displayed on the figure for comparison only.

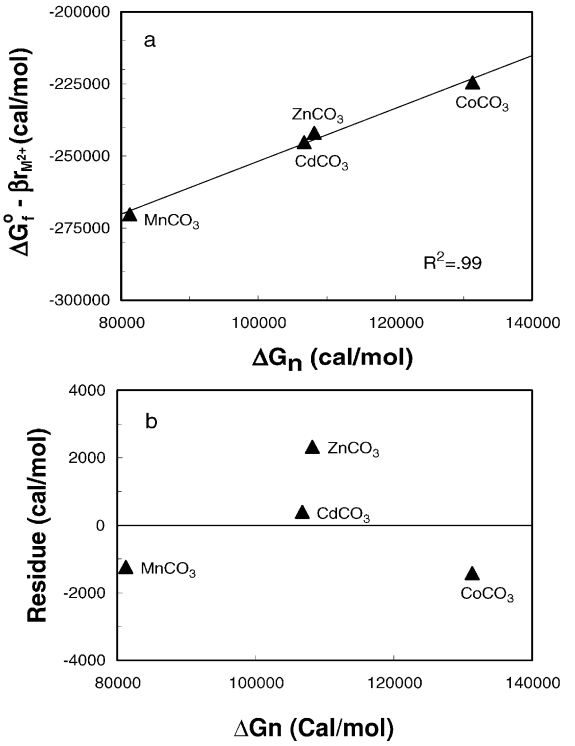

Fig. 3. (a) Multiple linear regression. The symbols represent experimentally derived values of the standard Gibbs free energies of formation for surface precipitates from Table 2. The vertical axis shows the left side of Eq. (1). (b) Residuals between experimentally derived G^{o}_{f} and values calculated from Eq. (21).

(Shannon, 1976), and $\Delta G^{o}_{n,\ M^{2+}}$ denotes the non-solvation contribution to the Gibbs free energy of formation of the aqueous M^{2+} ion (Helgeson et al., 1981). The coefficients in Eqs. (20) and (21) are regression parameters obtained from the regression of free energies listed in Tables 1 and 2. Figs. 2a and 3a show the regression results. Note that the correlations are statistically significant (R^2=0.99, see Table 3). For the HFO components, the average absolute residual is 2.6 kcal/mol (see Fig. 2b). Considering the metastable nature of HFO precipitates, this discrepancy is not surprising. A better agreement of estimated and experimental results is found for calcite surface precipitates. The average residual is about 1.4 kcal/mol (see Fig. 3b).

These correlations allow us to predict, to a first approximation, the Gibbs free energies of formation for end-members, for which there are no available

Table 3
Summary of regression analysis

Sorbent	a_{MX} (kcal/mol)	b_{MX} (kcal/mol)	β_{MX} (kcal/mol)	R^2
HFO	1.03266	−305.368	77.210	0.99
	(0.07548)	(20.316)	(15.726)	
Calcite	0.91500	−343.331	83.991	0.99
	(0.09124)	(20.953)	(18.825)	

The correlation takes the form of $\Delta G^{o}_{f,\,MX}-\beta_{MX}r_{M^{2+}}=a_{MX}\Delta G^{o}_{n,\,m^{2+}}+b_{MX}$.
Standard errors are given in parentheses.

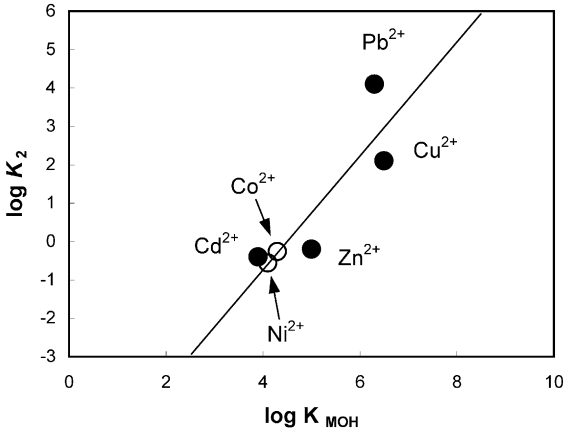

Fig. 4. Correlation of log K_2 (for reaction (2)) with first hydrolysis constants. The fitted line has a slope of 1.477 and intercept of 6.613. R^2=0.71. Solid symbols denote log K_2 derived from experimental data by Farley et al. (1985); open symbols are predicted values using this linear relationship. Log K_{MOH} values are from Dzombak and Morel (1990).

experimental data. Values of $G^{o}_{n,\,M^{2+}}$ and r for various metal ions are from Sverjensky and Molling (1992) and Shannon (1976), respectively. Table 4 shows the results.

These free energy values, in turn, permit calculation of equilibrium constants for surface precipitation reactions (3) and (15) for HFO and calcite, respectively. The Gibbs free energies of reactions (3) and (15) were calculated using the estimated free energies of formation for surface precipitates in this study and Gibbs free energy of formation for aqueous metal ions and water from Shock and Helgeson (1988). Equilibrium constants were then calculated from Eq. (12). Table 4 lists the results.

It is not meaningful to compare the predicted free energy for a "fictitious" $M(OH)_2$ component to that of its respective bulk solid because they represent different thermodynamic entities. However, some MCO_3(s) have calcite-type structures. Nevertheless, our predicted values for free energy are several kcal/mol lower than either experimentally derived values or values predicted for crystalline bulk carbonates. Part of this discrepancy may be due to the de facto Henrian standard state in the log K values from Comans and Middelburg (1987), who assumed an ideal solid solution and worked with experimental data in presumably dilute MCO_3(s) regions. However, most of the discrepancy probably may be explained by the definition of mole fraction for MCO_3(s). Comans and Middelburg (1987) used the total precipitated $CaCO_3$(s) in calculating mole fractions in the

Table 4
Estimated equilibrium constants and free energies for modeling surface precipitation

Component	Metal	Be	Mg	Ca	Mn	Co	Sr	Ni
$M(OH)_2$	$\Delta G^{o\dagger}_f$	−182,610	−211,599	−239,342	−158,142	−112,979	−241,012	−110,002
	Log $K^{\ddagger}$	−15.1	−7.8	−4.5	−7.6	−9.8	−4.5	−10.5
MCO_3	$\Delta G^{o\dagger}_f$	−227,550	−249,031	−269,250			−268,238	−159,320
	Log $K^{\S}$	−1.86	−0.06	−2.31			−4.23	5.95

Component	Metal	Sn	Ba	Eu	Ra	Pb	Hg	Cu	UO_2
$M(OH)_2$	$\Delta G^{o\dagger}_f$	−109,914	−238,292	−236,202	−239,415				−335,083
	Log $K^{\ddagger}$	−7.4	−5.7	−4.6	−6.0				−4.4
MCO_3	$\Delta G^{o\dagger}_f$	−152,856	−262,713	−263,820	−263,240	−150,801	−213,432	−135,271	−357,915
	Log $K^{\S}$	4.36	−7.55	−4.08	−8.24	3.53	−3.88	−8.30	−7.38

† At 25 °C and 1 bar, values in cal/mol.
‡ For reactions: $M^{2+}+2H_2O=M(OH)_2(s)+2H^+$.
§ For reactions: $M^{2+}+HCO_3^-=M(CO)_3(s)+H^+$.

surface precipitate. If only the first a few layers on the surfaces are involved in the surface precipitation (Davis et al., 1987), much larger mole fractions of MCO_3(s) would be calculated. That would result in much smaller experimentally derived log K values. Comparison of log K values calculated using free energy of formation for bulk carbonates from Sverjensky and Molling (1992) and values for Mn^{2+}, Cd^{2+}, Co^{2+}, and Zn^{2+} determined by Comans and Middelburg (1987) show a discrepancy of 3 to 6 log units. In other words, it could be that only from 1.5×10^{-5}% (for Co) to 0.07% (for Zn) of total $CaCO_3$ participates in the surface precipitation. Dzombak and Morel (1990) noted that, for crystalline solids, a reduced amount of sorbent should be used in mole fraction calculations. However, for amorphous iron hydroxide, the surface area to mass ratio is high, and the choice of mole fraction in the calculations may be less critical. Deciding which fraction of a total sorbent participates in surface precipitation can prove to be difficult. Katz and Hayes (1995) treated it as a fitting parameter and found 2% of total aluminum added best fit the Co^{2+} sorption onto α-Al_2O_3 data.

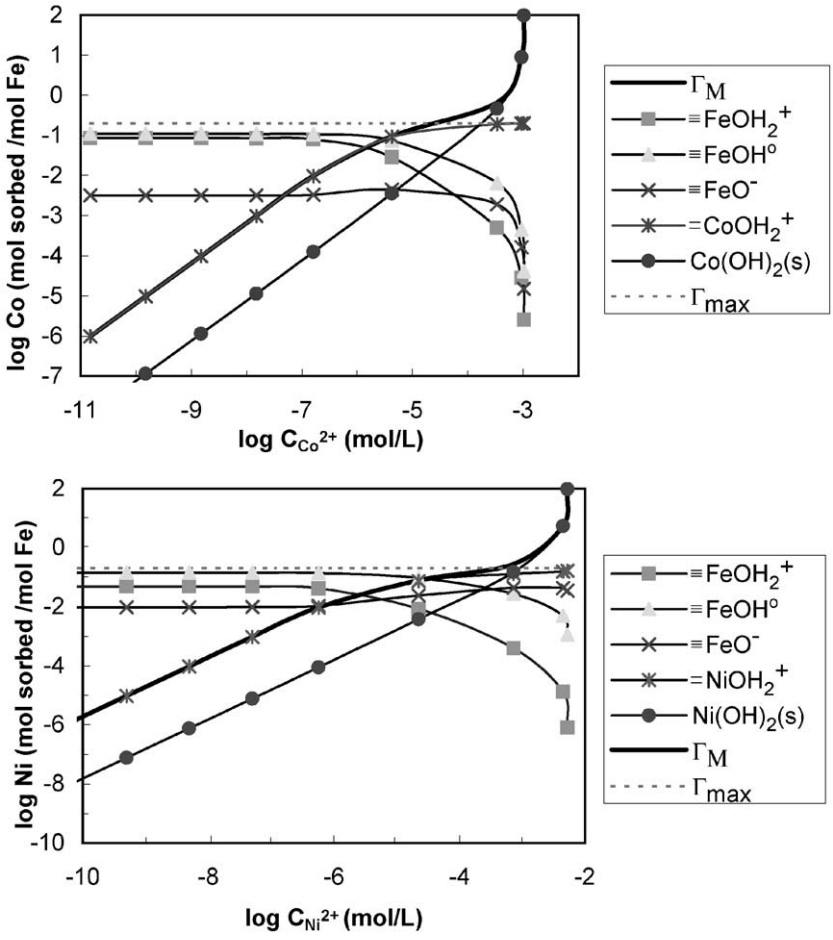

Fig. 5. Calculated isotherms for sorption of Co^{2+} and Ni^{2+} onto HFO with the surface precipitation model. The solution chemistry conditions are pH 6.5, I=0. 1 M (1:1 electrolyte), and TOTFe of 1 mM. Site density is assumed to be 0.2 mol/mol Fe (labeled as "Γ_{max}"). The vertical axis shows the concentrations of individual surface species as well as total metal adsorbed on surfaces (Γ_M defined in Fig. 1). The horizontal axis shows the "free" metal ion concentrations.

4. Applications

To illustrate the utility of the results in this study, the surface precipitation model is used to predict the sorption of Co^{2+} and Ni^{2+} onto HFO, for which there are no experimental data available at high sorbate/sorbent ratios. The solution chemistry is pH 6.5 and a 0.1 M, 1:1 electrolyte (inert) solution. The total Fe(III) concentration is 1.0×10^{-3} M. Values of the specific surface area, surface density for the "weak" site, and surface acidity constants from Dzombak and Morel (1990) are adopted in the calculation. First and second metal hydrolysis constants are taken from the database of Geochemist's Workbench© (Bethke, 1994). The hydrolysis constants for Fe^{3+} are from Stumm and Morgan (1996). The computer program FITEQL 4.0 (Herbelin and Westall, 1999) is used for the calculations of the complete surface precipitation model.

To model surface precipitation, we also need the log K for reaction (2). Farley et al. (1985) gave values for Pb^{2+}, Cd^{2+}, Cu^{2+}, and Zn^{2+}. These log K values appear to correlate linearly with the first hydrolysis constants of the respective metals (Fig. 4), in a similar fashion as for the surface complexation constants (cf. Fig. 10.1 and 10.2 of Dzombak and Morel, 1990). Using the relation in Fig. 4, log K_2 for Co^{2+} and Ni^{2+} are predicted to be -0.26 and -0.56, respectively. These values are then input into FITEQL for modeling.

Fig. 5 shows the calculated sorption isotherms for the surface precipitation of Co^{2+} and Ni^{2+}. Surface complexation dominates sorption at low dissolved metal concentrations. At higher dissolved metal concentrations, Co^{2+} and Ni^{2+} approach the maximum site concentrations in the system (0.2 mol/mol HFO). However, because the surface precipitation model is included, the plateau of site saturation does not occur. Rather, sorption increases as the solution approaches the solubility of the end-member component $Co(OH)_2(s)$ or $Ni(OH)_2(s)$. At high sorbate concentrations, where site saturation is approached, surface precipitation is the dominant mechanism of sorption. However, although model calculations continue to the saturation of end-member $Co(OH)_2(s)$ and $Ni(OH)_2(s)$, it should be noted that the ideal solid solution model is most likely only valid at low mole fractions of $Co(OH)_2(s)$ and $Ni(OH)_2(s)$.

5. Concluding remarks

In summary, the statistically significant correlations show that experimentally derived surface precipitation constants based on the surface complexation model are coherent with each other, lending support to the theoretical construct of the model (see Dzombak and Morel, 1990). Surface precipitation is important to model quantitatively metal uptake from aqueous solutions at high metal concentrations. The estimation of equilibrium constants for a large number of divalent metals facilitates the application of the surface precipitation model at high surface coverage.

Acknowledgements

Although the research described in this article has been funded wholly or in part by US Environmental Protection Agency; it has not been subject to the Agency's review and therefore does not necessarily reflect the views of the Agency, and no official endorsement should be inferred. Funding is also acknowledged from the National Science Foundation (EAR-0003816) ORISE, IGPP and from the Provost's Office at the University of Pittsburgh. Enlightened discussions with David Dzombak, as well as review comments from John Bargar, Pat Brady, and Eric Oelkers, have resulted in improvement of the manuscript. Various assistance from Dana McClish and Adam Nagle is appreciated. **[EO]**

References

Benjamin, M.M., 1978. PhD Thesis, Stanford University, Stanford, CA.

Bethke, C.M., 1994. Geochemist's Workbench, version 2.0, A User's Guide to Rxn, Act2, Tact, React, and Gtplot. Hydrogeology Program, University of Illinois.

Charlet, L., Manceau, A., 1992. X-ray absorption spectroscopic study of the sorption of Cr(III) at the oxide water interface: 2. Adsorption, coprecipitation, and surface precipitation on hydrous ferric-oxide. J. Colloid Interface Sci. 148, 443–470.

Comans, R.N.J., Middelburg, J.J., 1987. Sorption of trace metals on calcite: applicability of the surface precipitation model. Geochim. Cosmochim. Acta 51, 2587–2591.

Davis, J.A., Fuller, C.C., Cook, A.D., 1987. A model for trace metal sorption processes at the calcite surface: adsorption of Cd^{2+} and subsequent solid solution formation. Geochim. Cosmochim. Acta 51, 1477–1490.

Dzombak, D., Morel, F.M.M., 1986. Sorption of cadmium on hydrous ferric oxide at high sorbate/sorbent ratios: equilibrium, kinetics, and modeling. J. Colloid Interface Sci. 112, 588–598.

Dzombak, D., Morel, F.M.M., 1990. Surface Complexation Modeling—Hydrous Ferric Oxide. Wiley, New York, p. 393.

Exner, O., 1988. Correlation Analysis of Chemical Data. Plenum, New York.

Farley, K.J., Dzombak, D.A., Morel, F.M.M., 1985. Surface precipitation model for the sorption of cations on metal oxides. J. Colloid Interface Sci. 106, 226–242.

Fenter, P., Geissbuhler, P., DiMasi, E., Srajer, G., Sorensen, L.B., Sturchio, N.C., 2002. Surface speciation of calcite observed in situ by high-resolution X-ray reflectivity. Geochim. Cosmochim. Acta 64, 1221–1228.

Ford, R.T., Kemner, K.M., Bertsch, P.M., 1999. Influence of sorbate-sorbent interactions on the crystallization kinetics of nickel- and lead-ferrihydrite coprecipitates. Geochim. Cosmochim. Acta 63 (1), 39–48.

Ganguly, J., Saxena, S.K., 1987. Mixtures and Mineral Reactions. Springer-Verlag, Berlin, New York, p. 291.

Helgeson, H.C., Kirkham, D.H., Flowers, G.C., 1981. Theoretical prediction of the thermodynamic behavior of aqueous electrolytes at high pressures and temperatures. IV. Calculation of activity coefficients, osmotic coefficients, and apparent molal and standard and relative properties to 5 kb and 600 C. Am. J. Sci. 281, 1249–1516.

Herbelin, A., Westall, J.C., 1999. FITEQL—A Computer program for Determination of Chemical Equilibrium Constants from Experimental Data Department of Chemistry, Oregon State University, Corvallis, OR Report 99-01. Version 4.0.

Karthikeyan, K.G., Elloitt, H.A., 1999. Role of surface precipitation in copper sorption by the hydrous oxides of iron and aluminum. J. Colloid Interface Sci. 220, 88–95.

Katz, L.E., Hayes, K.F., 1995. Surface complexation modeling: II Stratigy for modeling polymer and precipitation reactions at high surface coverage. J. Colloid Interface Sci. 170, 491–501.

Lippmann, F., 1980. Phase equilibrium depicting aqueous solubility of binary systems. Neues Jahrb. Mineral. 139, 1–25.

Shannon, R.D., 1976. Revised effective ionic radii and systematic studies of interatomic distances in halides and chalcogenides. Acta Crystallogr. A 32, 751–767.

Shock, E.L., Helgeson, H.C., 1988. Calculation of the thermodynamic and transport properties of aqueous species at high temperatures: correlation algorithms for ionic species and equation of state predictions to 5 Kb and 1000 C. Geochim. Cosmochim. Acta 52, 2009–2036.

Sposito, G., 1984. The Surface Chemistry of Soils. Oxford Univ. Press, New York.

Stipp, S.L.S., 1999. Toward a conceptual model of the calcite surface: hydration, hydrolysis, and surface potential. Geochim. Cosmoschim. Acta 63, 3121–3131.

Stumm, W., 1992. Chemistry of Solid–Water Interfaces: Processes at the Mineral–Water and Particle–Water Interface in Natural Systems. Wiley, New York.

Stumm, W., Morgan, J., 1981. Aquatic Chemistry—Chemical Equilibria and Rates in Natural Waters. Wiley, New York.

Stumm, W., Morgan, J., 1996. Aquatic Chemistry—Chemical Equilibria and Rates in Natural Waters, 2nd edn. Wiley, New York.

Sturchio, N.C., et al., 1997. Lead adsorption at the calcite–water interface: synchrontron X-ray standing wave and X-ray reflectivity studies. Geochim. Cosmochim. Acta 61, 251–263.

Sverjensky, D.A., Molling, P.A., 1992. A linear free energy relationship for crystalline solids and aqueous ions. Nature 356, 231–234.

Towle, S.N., Bargars, J.R., Brown Jr., G.E., Parks, G.A., 1997. Surface precipitation of Co(II)(aq) on Al_2O_3. J. Colloid Interface Sci. 187, 62–82.

Wang, Y., Xu, H., 2000. Thermodynamic stability of actinide pyrochlore minerals in deep geologic repository environments. Materials Research Society Symposium Proceedings, Scientific Basis for Nuclear Waste Management, vol. XXIII, pp. 367–372.

Wang, Y., Xu, H., 2001. Precipitation of trace metal partitioning between minerals and aqueous solutions: a linear free energy correlation approach. Geochim. Cosmochim. Acta 65, 1529–1543.

Wells, P.R., 1968. Linear Free Energy Relationships. Academic Press, London.

Wells, A.F., 1984. Structural Inorganic Chemistry, 5th edn. Oxford Univ. Press, Oxford, p. 1382.

Xu, H., Wang, Y., 1999a. Use of linear free energy relationship to predict Gibbs free energy of formation of zirconolite phases ($MZrTi_2O_7$ and $MhfTi_2O_7$). J. Nucl. Mater. 275, 211–215.

Xu, H., Wang, Y., 1999b. Use of linear free energy relationship to predict Gibbs free energy of formation of pyrochlore phases ($CaMTi_2O_7$). J. Nucl. Mater. 275, 216–220.

Xu, H., Wang, Y., 1999c. Use of linear free energy relationship to predict Gibbs free energy of formation of MUO_4 phases. Radiochim. Acta 87, 37–40.

Xu, H., Ewang, Y., Barton, L., 1999. Application of a linear free energy relationship to crystalline solids MO_2 and $M(OH)_4$ phases. J. Nucl. Mater. 273, 343–346.

Zhu, C., Sverjensky, D.A., 1992. F–Cl–OH partitioning between apatite and biotite. Geochim. Cosmochim. Acta 56, 3435–3467.

Zhu, C., Sanders, S., Rafal, M., 1993. Modeling coprecipitation reactions as the control of trace elements mobility in groundwater. Geological Society of America Abstr. with Programs, vol. 25, No. 6, A-376.

Zhu, C., Yeh, G.-T., Waddell, R.K., 1996. A new approach to modeling metal contaminant transport associated with mining wastes. Proceedings of Tailings and Mining Waste '96, January 16–19, 1996. Colorado State University, Fort Collins, CO, pp. 341–350.